Performance and Condition Monitoring of Tidal Stream Turbines

Roger I. Grosvenor[1], Paul W. Prickett1[1], Carwyn Frost[1] and Matthew Allmark[1]

[1]Cardiff Marine Energy Research Group (CMERG), *School of Engineering, Cardiff University, Cardiff, South Glamorgan, CF24 3AA, Wales, UK*

grosvenor@cf.ac.uk
prickett@cf.ac.uk
FrostC1@cardiff.ac.uk
AllmarkMJ1@cardiff.ac.uk

ABSTRACT

Research within the Cardiff Marine Energy Research Group (CMERG) has considered the integrated mathematical modelling of Tidal Stream Turbines (TST). The modelling studies are briefly reviewed. This paper concentrates on the experimental validation testing of small TST models in a water flume facility. The dataset of results, and in particular the measured axial thrust signals are analysed via time-frequency methods. For the 0.5 m diameter TST the recorded angular velocity typically varies by ± 2.5% during the 90 second test durations. Modelling results confirm the expectations for the thrust signal spectrums, for both optimum and deliberately offset blade results. A discussion of the need to consider operating conditions, condition monitoring sub-system refinements and the direction of prognostic methods development, is provided.

1. INTRODUCTION

Research within the Cardiff Marine Energy Research Group (CMERG) has established a series of generic design guidelines for the developing commercial deployment of Tidal Stream Turbines (TST). Design considerations were reported by O'Doherty, Mason-Jones, O'Doherty, Evans, Woolridge and Fryett (2009). The mathematical models combine Computational Fluid Dynamics (CFD), structural Finite Element Analysis (FEA) to provide Fluid-Structure-Interaction (FSI) results. Non-dimensionalised power and thrust curves, along with flow visualisations, are produced for a variety of configurations and flow conditions. The non-dimensionalised research was reported by Mason-Jones, O'Doherty, Morris, O'Doherty, Byrne, Prickett, Grosvenor, Owen, Tedds and Poole (2012).The progress and outputs of the modelling studies are briefly reviewed in section 1.1.

The mathematical models are validated via the testing of scale model (0.5 m diameter) turbines in a water flume facility at Liverpool University. A dataset of results was available for a particular set of performance and monitoring evaluation tests. For these a three blade turbine was used, with a constant plug flow of 0.94 m.s-1 and at a range of controlled conditions within the power curve profiles. Previous studies and testing had compared results for designs with varying numbers of blades and had confirmed the optimum blade angle setting for the 3 blade option. Recent studies have used profiled flow conditions and with the addition of surface waves.

For the dataset considered in this paper, the recorded signals were angular velocity, servo motor current (used to oppose flow generated motion and hence to estimate generated power) and the overall axial thrust. Tests were split between an 'optimum' setup (three identical blade angles) and an 'offset' setup. For the latter, one of the three blades was deliberately set at other than its optimum pitch angle. This condition was deemed to represent potential blade faults, whereby one damaged or deteriorated blade would contribute less than usual to the generated power output. From a condition monitoring viewpoint such deviations in performance were expected to also be detectable in the more accessible axial thrust signals.

The experimental signals are described in detail in section 3, along with the limitations of the signals, with respect to time-frequency analysis (section 4).

In section 4, traditional frequency spectrum plots are initially presented. The frequency spectrums obtained included components, for any given set of test conditions, observed at the rotational frequency (ω_r) and at either or both $2.\omega_r$ and $3.\omega_r$. Thrust measurements, from the turbine supporting structure, are more easily made in comparison at rotating elements and their potential to form a constituent part of an integrated TST monitoring system is explored.

With the aim of more robust detection of individual blade problems, methods of improving the frequency spectrum resolutions were required. In particular synchrosqueezing time-frequency methods were assessed and are presented in section 4.4.

1.1. Review

Tidal energy can provide a highly predictable and sustainable level of energy. One of the emerging technologies is the use of submerged tidal stream turbines (TST), which for example, may be seabed mounted. UK tidal stream technologies are increasingly being installed and tested as full-scale devices. The first example was the Marine Current Turbines (MCT) 11m diameter, 2 blade horizontal axis Seaflow device. The 300 kW capability from a tidal flow of approximately 2.8 ms^{-1} has increased to 1.2 MW for the subsequent SeaGen project. TST technologies are rapidly developing, different designs are being proposed, and experimental performance testing is also carried out at small scale, with support from sophisticated mathematical modelling. A review of research progress is provided by Ng, Lam and Ng (2013).

1.2. Modelling

For horizontal axis tidal turbines (HATT) the computational fluid dynamics (CFD) models have been considered in a non-dimensionalised manner and have led to generic power and thrust performance curves for use by designers. The non-dimensional performance curves were validated via experimental testing at the water flume facility in Liverpool University.

Figure 1 [Myers and Bahaj (2012)] shows the general arrangement for a HATT installation and summarises the main parameters and effects of interest.
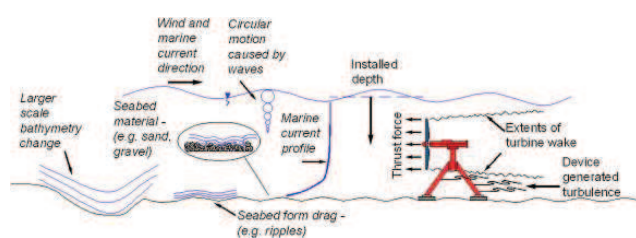

Figure 1. Horizontal Axis Tidal Turbine (HATT) [Myers & Bahaj (2012)]

The CFD models have been extended to include Fluid-Structure Interactions (FSI). Accordingly the 2 way coupling between fluid flows and structural deflections are used to improve the simulation results for realistic flow and installation conditions. The experimental testing has also been developed to allow profiled flow testing, in addition to the original plug flow testing. The addition of surface waves

has also been developed for the water flume facility at Liverpool University.

The experimental testing to validate the range of mathematical modelling activities has provided an opportunity to assess potential condition monitoring and prognostics methods. Of particular relevance, to such aspects reported in this paper, are models used to investigate the interactions between the turbine blades and the supporting structures. There are observable shadow effects as the blades pass in front of the supporting structure. As will be reported in section 4.1, cyclic variations in the axial thrusts are produced as a consequence of such effects. It is the cyclic variations that are investigated, with frequency domain and time-frequency domain methods, as an potential contributing sub-system to a TST condition monitoring system. The modelled effects have been reported by Mason-Jones, O'Doherty, Morris and O'Doherty (2013). The contributions of such models are reported in section 4.

1.3. Condition Monitoring & Prognostics

Condition monitoring and fault diagnosis is considered to be elemental in developing marine current turbine energy extraction. Tidal energy technology has yet to be proven with regard to long term operational availability and reliability. It is accepted that the harsh marine environments and problems with accessibility for maintenance may exasperate availability and reliability problems. Bahaj (2011) noted that minimising uncertainty surrounding the operation and maintenance of such devices will be crucial in improving investor confidence and achieving economically viable power extraction. Experience within the wind energy sector, for example as reported by Hameed, Ahn and Cho (2010), Yang, Tavner, Crabtree and Wilkinson (2010) and Tian and Jin (2011), has suggested that online condition monitoring and fault detection could minimise maintenance costs and improve availability of the energy extraction technology. As such condition monitoring and fault diagnosis hardware and software architectures should at this stage seek to be general and adaptable

Figure 2 [Grosvenor and Prickett (2011)] outlines constituent components for such a generalised TST monitoring system. The investigations reported in this paper focus on the use of supporting structure based sensors. In particular, the potential of time-frequency analysis methods applied to the background cyclic variations in the supporting structure are considered.

2. EXPERIMENTAL TESTING

A series of scale model turbines have been developed by the CMERG group for water flume testing. For the tests reported and analysed in this paper a 0.5 m diameter, 3

blade turbine was used. Each blade pitch angle was adjustable and from previous testing, not reported here, the optimum blade pitch angle had been determined to be 6° for the configuration in use. This prior testing information was also utilized to simulate a blade fault. In this case one of the blades was deliberately offset, to a pitch angle of 15°.
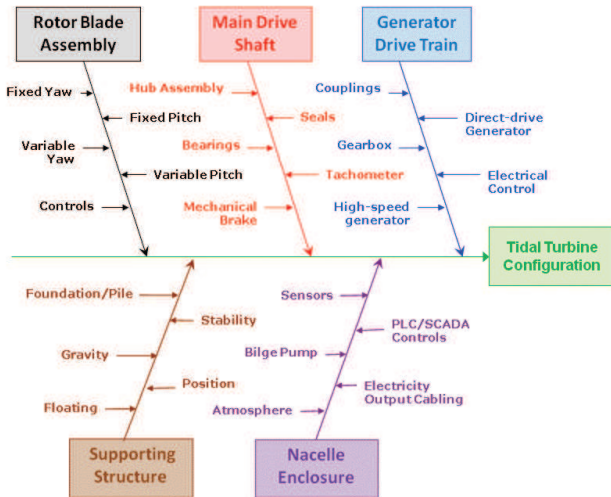

Figure 2. Constituents of a Generalised TST Monitoring System.

The water flume was configured and operated to provide plug flow conditions (constant flow with water depth) and an average axial flow velocity of 0.94 m.s^{-1}.

A direct drive servo motor was used to generate controllable torques in opposition to those from the flow and turbine blades. Accordingly tests were achievable for a range of conditions from within the turbine performance curve. These ranged from the peak power conditions down to the free-wheeling condition with negligible power output. These were classified by a percentage of maximum torque measure, with 19 settings ranging from 45% downwards in 2.5% steps to 0% of maximum torque. The servo motor was capable of delivering a maximum torque of approximately 4.92 Nm. As stated, the tests were performed for both optimum blade settings (6°-6°-6°) and with one blade deliberately offset (6°-15°-6°).

For each individual test data was recorded for between 90 and 150 s. The recorded signals consisted of the servo motor current (used to calculate power outputs), the angular velocity of the turbine and the total axial thrust.

Figure 3 show the general setup for the water flume tests. The junction between the vertical turbine support tube and the horizontal supporting frame was fitted with a force block. The strain gauge arrangement of the force block enabled the measurement of the total axial thrust.

3. EXISTING DATASETS

Accordingly the analysed dataset consisted of a total of 38 test cases, equally split between optimum blade and offset blade setups. Figure 4 summarises the test configurations for the turbine power curves.
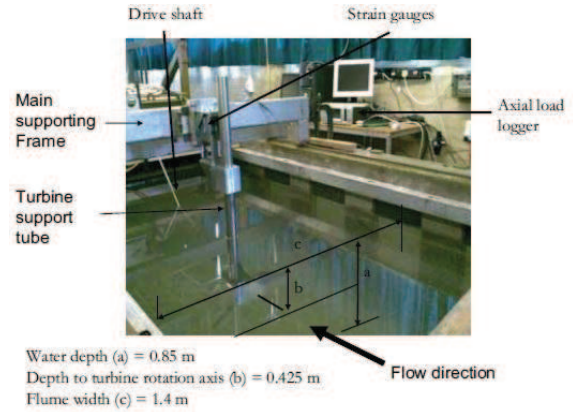

Figure 3. Liverpool University Water Flume and Experimental Setup.

These are plotted as power coefficient, C_p, vs tip speed ratio, TSR. The former is the ratio of actual power compared to theoretical power. TSR is a normalized measure, for a given turbine, of the angular velocity. The performance reducing effect of the one offset blade is evident.
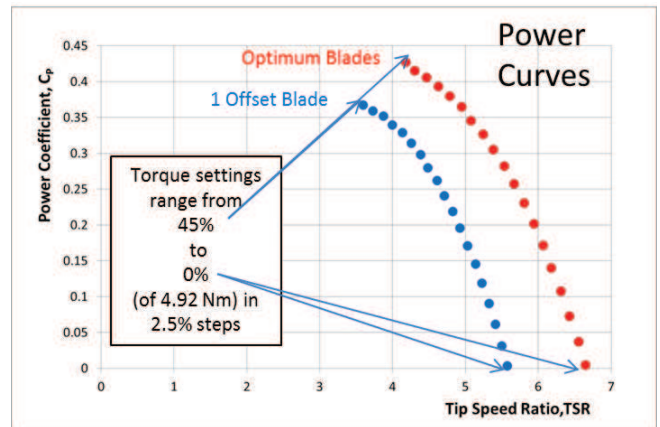

Figure 4. Power Curves for Experimental Datasets

Example results are shown in Figure 5. The upper plot shows the thrust signal variations during a 90 s test for optimum and offset blade cases, for 30% and 32.5% torque settings. The lower plots shows the angular velocity fluctuations for the same cases.
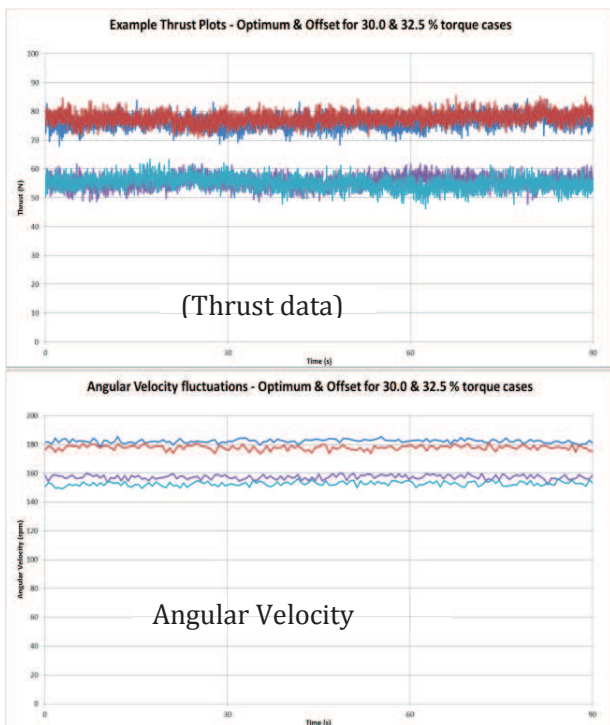
Figure 5. Example Experimental Results: Axial Thrust and Angular Velocity Signals for Optimum and Offset Cases.

Figure 6 shows an extract of the datasets of Figure 5. The zoomed time axis is equivalent to approximately 5 turbine rotations for the conditions considered..
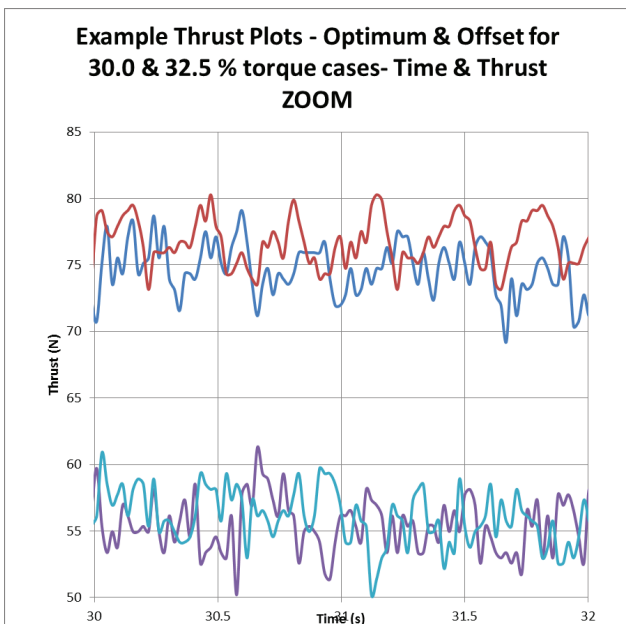

Figure 6. Zoomed Axial Thrust and Angular Velocity Signals

There are some cyclic variations apparent in the signals and these observations were the basis for the time-frequency analyses.

The datasets were not ideal for such analysis methods. The axial thrust was sampled at approximately 47.6 Hz. The angular velocity was sampled at only 1.75 Hz. For any particular test case there was also evidence of quantisation effects in the digitized thrust signals.

For the range of conditions in the 38 datasets the 90 s recordings represented between 192 and 359 turbine rotations, for angular velocities between 128 and 239 rev.min^{-1}. When the analysis is aimed to provide information per blade per revolution these characteristics potentially pose considerable limitations.

In commercial installations the TST power generation will be controlled to produce the maximum power within the prevailing flow conditions and constraints. For the condition monitoring approaches to be applicable they need to be insensitive and/or adapt to the prevailing flow conditions. The datasets spanning a range of angular velocities, and hence TSRs, for in this case a fixed flow velocity were utilised to assess this aspect.

4. ANALYSIS

4.1. Axial Thrust Modelling

Figure 7 shows the steady-state output from a CFD model used to predict the constituent and total thrust for a HATT. The CFD results shown are for a 3 bladed full size (10 m diameter) turbine, with the blades set at optimum pitch angles. Plug flow with a velocity of 3.086 ms^{-1} was used with operating conditions pertaining to a TSR of 3.61.
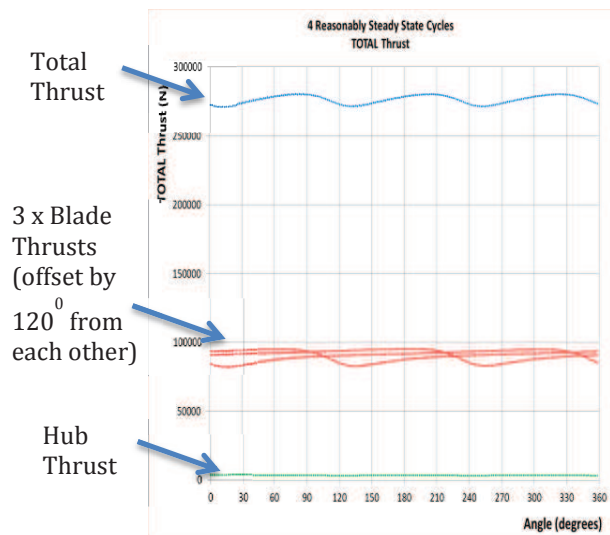

Figure 7. CFD Modelling of Thrusts

For the full size turbine the latter equates to an angular velocity of 21.3 rev.min^{-1}.

The thrust models were developed for the ANSYS fluid flow (CFX) platform. The fluid domain box was 50 m square and 150 m long and was established with appropriate plug flow boundary conditions. The mesh, for the multiform reference form (MRF) cylinder, of 12 m diameter and 4.5 m length, (surrounding the 3 bladed turbine model), consisted of 4.6 M cells.

The models are computationally intensive and settle to give steady state results. Figure 7 shows the thrust components for 1 turbine revolution. As expected the blade effects, passing and shadowing the support tube, are offset by 120° from each other. The small contribution, from the flow impinging on the hub, is not included in the time-frequency analysis. The total axial thrust displays relatively small cyclic variations, when compared to the mean axial thrust. Figure 8 shows the thrust profile for 3 blades for 2 turbine revolutions.
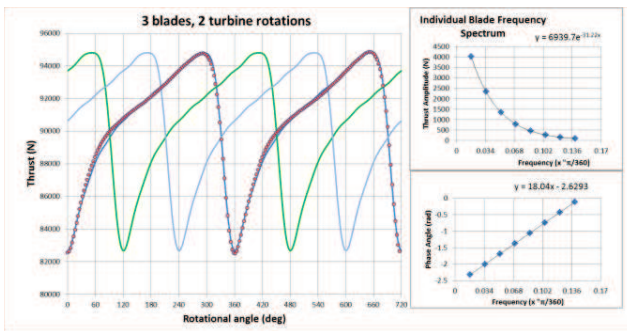

Figure 8. CFM Model of Blade Thrusts and Individual Blade Frequency Spectrum.

Figure 8 also shows the frequency spectrum for an individual blade, for 8 constituent terms all of which are at multiples of the fundamental frequency. The average thrust value is not plotted.

4.2. Frequency Analysis

The 38 experimental datasets were initially analysed by using standard Fast Fourier Transform (FFT) functions with the Matlab environment. The obtained spectrums were investigated to determine whether differences between the optimum blade and offset blade subsets were reliably detectable. Figure 9 shows a composite waterfall spectrum plot, for the 19 optimum blade tests. The percentage of maximum servo motor torques ranged from 0% (freewheeling) to 45% (close to peak power generation). The frequency spectrums are shown as amplitude^2 plots.
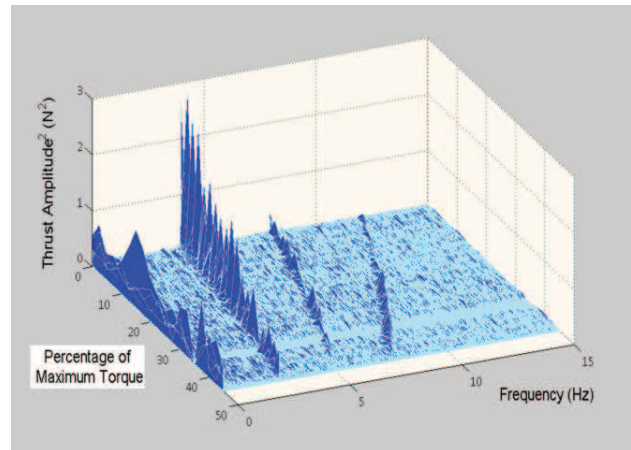

Figure 9. Waterfall Thrust Amplitude^2 Frequency Spectrum for 19 Optimum Blades Tests.

The rotational frequency (ω_r) was readily detectable, from the total axial thrust signals, and strongly correlated with the recorded angular velocities. For the optimum blade results shown the ω_r values ranged from 2.50 to 3.98 Hz. These are in accordance with the mean angular velocities, that ranged from 150 to 239 rev.min^{-1}. The harmonics, 2.ω_r and 3.ω_r were generally detectable. The 3.ω_r components were expected (discussed in section 5.1) and are in agreement with the thrust modelling exercise. There were some potential differences in the patterns observed for 2.ω_r components when comparing optimum blade and offset blade results. The discussed data limitations and the time varying turbine rotational velocities during testing were deemed to reduce the clarity of such observations. Accordingly the angular velocity fluctuations were analysed and time-frequency methods were utilised.

4.3. Angular Velocity Fluctuations

The 38 datasets were subjected to simple statistical analysis. Figure 5 (section 3) is an example of typical time domain angular velocity data. For the optimum blade tests the typical fluctuations were found to be ± 2% of mean values. For the offset blade test the fluctuations were generally larger and a typical value was ± 2.5% of mean values.

4.4. Time-Frequency Analysis

In light of the angular velocity analysis the spectrogram function within Matlab was used to obtain time-frequency plots. By optimizing the spectrogram parameters, including the number of FFT points, the overlap extent and windowing, the plots typically provided observable ω_r, 2.ω_r and 3.ω_r components. Due to the dataset limitations the spectrogram plots were not obtainable with sufficient resolution in either the time or frequency axes, and are not presented here.

Other approaches, including order analysis and time series analysis are also currently being investigated, and are not reported. Rather, the application of an emerging time-frequency method known as synchrosqueezing is assessed for the turbine data.

A small number of research groups have developed and reported on the synchrosqueezing, and have made available toolkits for use within Matlab. Iatsenko, McClintock and Stefanovska (2013) reported on one such toolkit. Reported applications include the condition monitoring and fault diagnosis of gearboxes. The latter was reported by Li and Liang (2012).

Iatsenko et al (2013) described synchrosqueezing as a nonlinear transformation of windowed Fourier transforms and wavelet transforms. Synchrosqueezing is used to increase the data concentration and allows for extraction and reconstruction of the analysed signals components. They made detailed comparisons with other methods, for a variety of test signal cases/types.

In the analysis reported here the Matlab toolkit developed at Lancaster University, and reported by Iatsenko et al (2013), was used. The algorithm may be applied to time domain signals, for which the sample rate is specified as an input parameter. Other parameters provide choices for the type and combinations of plots that are produced. To reduce the computational overheads either or both minimum and maximum frequencies of interest can be specified.

A parameter 'f0' has a unity default value. However by varying the value of 'f0' resolution of the overall frequency spectrum results can be improved. Alternatively 'f0' may be used to improve the time resolution, at the expense of the spectrum resolution. The latter was found to provide determination of the time-varying rotational frequency due to velocity fluctuations.

Iatsenko et al. (2013) reported that 'f0' is a critical value in time-frequency analysis and confirm that it determines a tradeoff between time and frequency resolutions. The optimal 'f0' setting depends of the signal analysed, however determining the time-frequency area of interest enables an automatic procedure for the selection of parameters within the algorithm.

The two plots that were utilized in analyzing the turbine data were (i) a coloured-coded time-frequency spectrogram plot and (ii) a time-averaged Synchronised Windowed Fourier Transform (SWFT) plot.

Figure 10 shows an example result for (i), for optimum blades at 30% torque. The sample rate was 47.6 Hz, the frequency range was set to 2.6 – 3.4 Hz and the 'f0' value was 0.75. For the 4286 samples in the 90 s thrust signals these settings produced 41 time distributed spectrums. The lower plot of Figure 10 shows a composite plot for the 41 spectrums obtained and the variations due to angular velocity changes.. The algorithm is shown to determine the variations in the rotational frequency, which is inversely proportional to the angular velocity fluctuations, during the test duration.
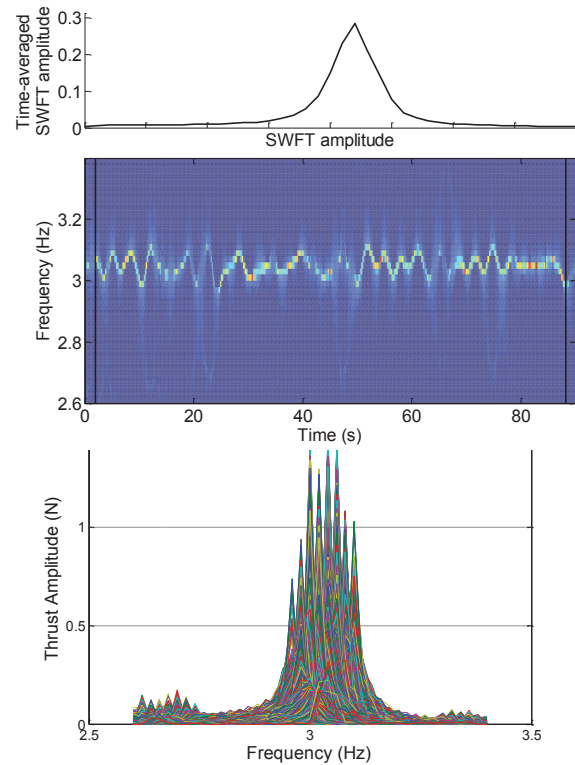

Figure 10. Synchrosqueezing Results for Optimum Blades at 30% of Maximum Torque.

The synchrosqueezing algorithm was also applied with different parameters in order to produce type (ii) plots, i.e. time averaged SWFT plots. In such cases the frequency range was set to 0 – 10 Hz and the 'f0' parameter was set as 2. Figure 11 shows comparative results obtained for 4 of the datasets. These examples are for the cases shown previously in Figure 5, i.e optimum and offset blades at 30% and 32.5% of maximum torque settings.

Figure 12 shows the spectrum results, for torque settings between 20 and 45%. For both the optimum blade and offset blade cases the rotational frequency, ω_r , was consistently detected. The variation in the amplitude of this component with the operating conditions, determined via the percentage torque settings, was consistent with the FFT results of Figure 9. However there is no consistent pattern for the $2.\omega_r$ and $3.\omega_r$ components. Neither is there any distinct difference for the optimum and offset datasets considered.

It is, for example, merely a coincidence that the spectrums of Figure 11 shows 3 main components for the optimum blade results used as examples and that only 2 main components are apparent for the offset blade examples.
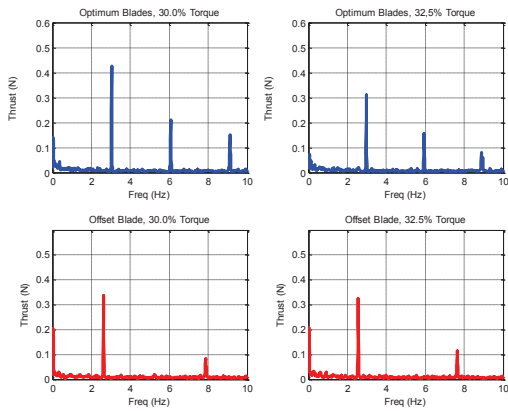
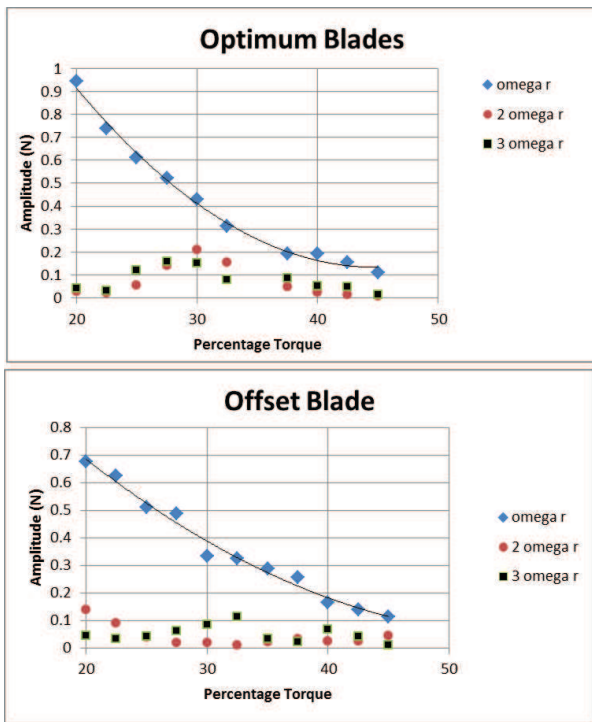Figure 11. Comparison of Thrust Amplitude Frequency Spectrum Results.

Figure 12. Comparison of Frequency Components for Optimum and Offset Blades.

There are benefits in using the synchrosqueezing toolbox; the time average spectrums produced show the harmonic components more distinctly. Conversely, with the settings used to produce Figure 10, the time varying angular velocities can be evaluated directly from the thrust signal.

Further insights into the spectrum results obtained with respect to the $2.\omega_r$ and $3.\omega_r$ components are provided in section 5. These emanate from an extension of the thrust

modelling. Such results are being produced by CMERG from further simulations using the blade thrust CFD models. These are not yet available, and an estimated approach is used in this paper to support the discussions.

5. DISCUSSION

5.1. Cyclic Axial Thrusts

Figure 8 (section 4.1) showed the CFD model blade thrusts for a full-scale 3 bladed TST, for 2 turbine rotations and with a zoomed thrust axis. The CFD model assumes that the blades are identical and that all geometries are appropriately symmetrical. This is reflected in the total axial thrust variations (now for 1 turbine rotation) shown in Figure 7 (section 4.1). Included in Figure 8, were the FFT computed frequency spectrum plots for an individual blade. In this discussion the FFT spectrum for the total thrust cyclic variations are now considered.

The upper plot of Figure 13 shows the thrust amplitude spectrum for the combined axial thrust values. As stated, perfect symmetries and setups pertain to the CFD simulations and the 3 blades are offset from each other by exactly 120°. Accordingly the frequency vectors from the 3 blades cancel each other out, except for those at $3.\omega_r$ and multiples thereof. This provides an immediate inconsistency with the spectrums for the experimental results.

The tolerances pertaining to the experimental scale-size model were thus considered. The manufacture of the turbine was to a high standard, however small eccentricity and other non-symmetries are likely. More particularly, the turbine was designed to have adjustable blade pitch angles. These were adjusted, and set as appropriate between tests, using a surface table and standard angle templates. There was some reliance on the skill and judgment of the experimenter.

To simulate this relatively small adjustment was made for one of the blades to create some asymmetry compared to the ideal case shown in Figure 8. For the results discussed here the adjustment consisted of a 10% reduction in the mean thrust level combined with a 10% reduction in the range of thrusts for blade 2. The FFT amplitude spectrum results then obtained for the total thrust are shown in the lower plot of Figure 13.

The difference is then that all ω_r, $2.\omega_r$ and $3.\omega_r$ components can be seen in the spectrum, and are in closer agreement with the experimental results.

The simulated adjustment in this example is small compared to the difference in thrust values that would apply for the deliberately offset blade. For the offset blade the change to a 15° pitch angle is far more substantial, if judged by the reduced power performance at such a setting, as was seen in Figure 4 (section 3).
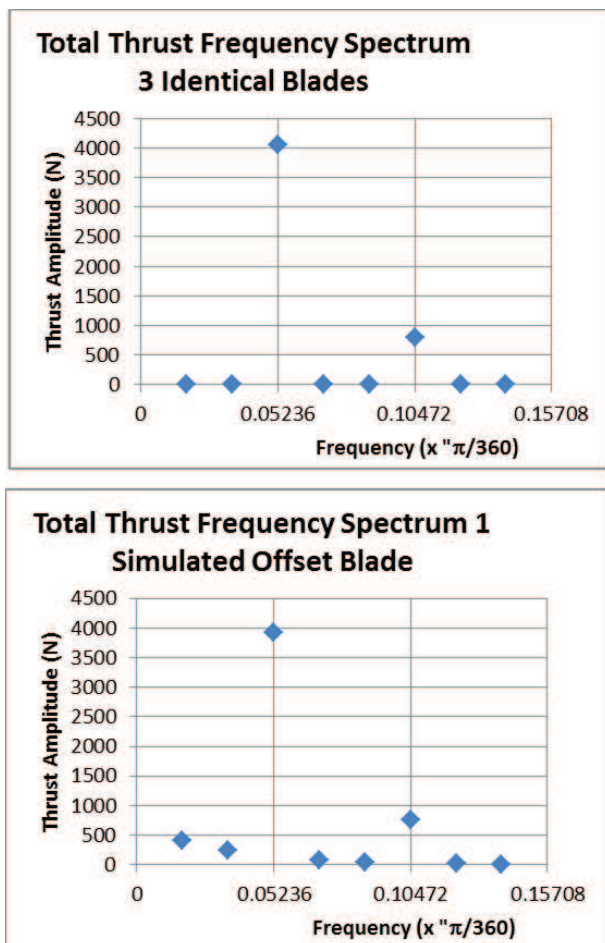
Figure 13. Comparison of Thrust Amplitude Frequency Spectrum for Symmetrical Blades and with Simulated Effects due to Tolerances.

5.2. Prognostics

The analysis of the potential use of one constituent of developing TST condition monitoring systems has been presented and discussed. The total thrusts acting on a TST support structure are more accessible than measurements from rotating elements. The latter will be vital for the monitoring systems and some developments towards this are discussed in section 5.3.

For the experimental datasets, with their far from ideal characteristics, there are results of interest from the time-frequency analyses. The synchrosqueezing methods improved the extraction of useful spectrum information from those datasets. In particular the angular velocity fluctuations were obtainable directly from the thrust signals.

The full-scale deployment of TSTs will inevitably mean that the operation and monitoring of each individual TST will be heavily site specific. The logging of operational conditions is a vital element of prognostic systems and the recording and analysis of structural thrust signals is believed to have a role to play in such systems.

5.3. Future Developments

The next generation of 0.5 m diameter scale-model TST is about to be deployed for water flume testing. The number of signals to be captured is to be extended, and the sample rates and resolution of the existing signals will be greatly improved. The additions include sensing of rotating components. A strain gauge based blade torque sensor has been developed. A 3-axis MEMS accelerometer has been included and the servo motor drive will provide an encoder output. The latter will improve the synchronization of recorded signals to turbine rotations. Researchers such as Bechhoefer, Wadham-Gagnon and Boucher (2012) have reported experiences with 3-axis MEMS accelerometers for wind turbine monitoring. Wider scale wind turbine performance monitoring has also been reported, for example by Uloyol and Parthasarathy (2012).

6. CONCLUSIONS

The use of support structure thrust signals as a constituent part of a TST monitoring system has been investigated. The limitations of the existing experimental datasets have been quantified and assessed. CFD models have been used to justify the cyclical patterns observed in the thrust signals. The models have been adapted to allow for manufacturing tolerances and small misalignments. These adaptations have enabled a closer correlation between the observed and modelled frequency components. The next generation of scale TSTs to be tested will provide more appropriate data characteristics. The longer term, site specific, monitoring of such signals will provide operating profile information for subsequent prognostics models.

REFERENCES

Bahaj, A.S., (2011), Development of marine current turbines for electricity production. *IEEE Power and Energy Society General Meeting,* July 2011 Detroit, pp. 1–4.

Bechhoefer, E., Wadham-Gagnon, M. & Boucher, B. (2012). Initial condition monitoring experience on a wind turbine. *Annual Conference of Prognostics and Health Management Society (pp 1 – 8),* September 23-27, Minneapolis.

Grosvenor, R.I. & Prickett, P.W. (2011). A discussion of the prognostics and health management aspects of embedded condition monitoring systems. *Annual Conference of Prognostics and Health Management Society (pp 1 – 8),* September 25-25, Montreal.

Hameed, Z., Ahn, S.H. & Cho, Y. M. (2010). Practical aspects of a condition monitoring system for a wind turbine with emphasis on its design, system architecture, testing and installation, *Renewable Energy*, vol. 35, no. 5, pp. 879–894.

Iatsenko, D., McClintock, P.V.E. & Stefanovska, A. (2013). Linear and synchrosqueezed time-frequency representations revisited. *Digital Signal Processing, arXiv:1310.7215v2 [math.NA] pp1-45*.

Li, C. & Liang, M. (2012). Time-frequency signal analysis for gearbox fault diagnosis using a generalized synchrosqueezing transform. *Mechanical Systems and Signal Processing*, vol 26, pp. 205 – 217. Doi:10.1016/j.ymssp2011.07.001.

Mason-Jones, A., O'Doherty, D.M., Morris, C.E., O'Doherty, T., Byrne, C.B., Prickett, P.W., Grosvenor, R.I., Owen, I., Tedds, S. & Poole, R.J. (2012). Non-dimensional scaling of tidal stream turbines. *Energy,* vol 44 pp. 820 – 829. doi: 10.1016/ j.energy.2012.05.010.

Mason-Jones, A., O'Doherty, D.M., Morris, C.E., & O'Doherty, T. (2013). Influence of a velocity profile and support structure on tidal stream turbine performance. *Renewable Energy*. Vol 52, pp. 23 – 30. Doi:10.1016/j.renene.2012.10.022.

Myers, L.E. & Bahaj, A.S. (2012). An experimental investigation simulating flow effects in first generation marine current energy converter arrays. *Renewable Energy*. Vol 37, pp. 28 – 36. Doi:10.1016/j.renene.2011.03.043.

Ng, K-W., Lam, W-H. & Ng, K-C. (2013). 2002-2013: 10 years of research progress in horizontal-axis marine current turbines. *Energies.* Vol 6, pp. 1497 – 1526. Doi:10.3390/en6031497.

O'Doherty, T., Mason-Jones, A., O'Doherty, D.M., Evans, P.S., Woolridge, C.F. & Fryett, I. (2009), Considerations of a horizontal axis tidal turbine. *Energy,* vol 163 (issue EN3), pp. 119 – 130.

Tian, Z. & Jin, T. (2011). Maintenance of wind turbine systems under continuous monitoring, *Reliability and Maintainability Symposium (RAMS),* pp. 1 –6.

Uluyol, O. & Parthasarathy, G. (2012). Multi-turbine associative model for wind tunnel performance monitoring. *Annual Conference of Prognostics and Health Management Society (pp 1 – 8),* September 23-27, Minneapolis.

Yang, W., Tavner, P. J., Crabtree, C. J. & Wilkinson, M. (2010). Cost-effective condition monitoring for wind turbines, *Industrial Electronics, IEEE Transactions on*, vol. 57, no. 1, pp. 263 –271.

BIOGRAPHIES

Dr Roger I. Grosvenor

Educated at Cardiff University obtaining a BEng Mechanical Engineering degree (1978), a MEng via fluid dynamics research (1981) and a PhD on the topic of in-process measurement of machined components (1994). He is currently a reader in systems engineering at Cardiff University and has been employed as a lecturer there since 1984. He has published 90 journal and conference papers, mainly on the topic of machine and process condition monitoring. He is co-director of the Intelligent Process monitoring & management (IPMM) centre. He is a chartered engineer and a member of the Institute of Measurement and Control.

Paul W. Prickett

Educated at Cardiff University obtaining a BEng degree in Mechanical Engineering (1979). He is a senior lecturer in Cardiff School of Engineering and is also a co-director of the IPMM centre (established in 1998). He has directed the work of sixteen researchers and has supervised seven PhD students and two EngD students. He has published over 70 papers on the topic of machine and process condition monitoring. He at presented at numerous conferences and acts as a referee for journals and funding bodies in his field of research. He is a chartered engineer and a member of the Institution of Mechanical Engineers.